frontiers in Earth Science

ORIGINAL RESEARCH
published: 13 April 2016
doi: 10.3389/feart.2016.00039

Internal Structure and Current Evolution of Very Small Debris-Covered Glacier Systems Located in Alpine Permafrost Environments

*Jean-Baptiste Bosson * and Christophe Lambiel*

Faculty of Geosciences and Environment, Institute of Earth Surface Dynamics, University of Lausanne, Lausanne, Switzerland

This contribution explores the internal structure of very small debris-covered glacier systems located in permafrost environments and their current dynamical responses to short-term climatic variations. Three systems were investigated with electrical resistivity tomography and dGPS monitoring over a 3-year period. Five distinct sectors are highlighted in each system: firn and bare-ice glacier, debris-covered glacier, heavily debris-covered glacier of low activity, rock glacier and ice-free debris. Decimetric to metric movements, related to ice ablation, internal deformation and basal sliding affect the glacial zones, which are mainly active in summer. Conversely, surface lowering is close to zero ($-0.04\,m\,yr^{-1}$) in the rock glaciers. Here, a constant and slow internal deformation was observed (*c.* $0.2\,m\,yr^{-1}$). Thus, these systems are affected by both direct and high magnitude responses and delayed and attenuated responses to climatic variations. This differential evolution appears mainly controlled by (1) the proportion of ice, debris and the presence of water in the ground, and (2) the thickness of the superficial debris layer.

Keywords: debris-covered glaciers, rock glaciers, permafrost, ground ice, electrical resistivity tomography, dGPS

OPEN ACCESS

Edited by:
Matthias Huss,
ETH Zurich, Switzerland

Reviewed by:
Sebastien Monnier,
Pontifical Catholic University of Valparaíso, Chile
Roberto Seppi,
University of Pavia, Italy

****Correspondence:***
Jean-Baptiste Bosson
jeanbaptiste.bosson@gmail.com

Specialty section:
This article was submitted to Cryospheric Sciences, a section of the journal Frontiers in Earth Science

Received: *05 January 2016*
Accepted: *29 March 2016*
Published: *13 April 2016*

Citation:
Bosson JB and Lambiel C (2016) Internal Structure and Current Evolution of Very Small Debris-Covered Glacier Systems Located in Alpine Permafrost Environments. Front. Earth Sci. 4:39. doi: 10.3389/feart.2016.00039

INTRODUCTION

Numerous positive and negative feedbacks characterize the current adaptation of glacier systems to climatic changes (WGMS, 2008; Haeberli et al., 2013). Among them, the accumulation of debris at the glacier surface by the emergence of englacial load and/or direct supraglacial deposition in high relief environments significantly impacts glacial dynamics (Benn et al., 2003). Indeed, depending on its thickness, the debris cover enhances or limits the ice ablation (Nicholson and Benn, 2006; Lambrecht et al., 2011). The melt rate increases below a few centimeters of thickness threshold (2–8 cm, e.g., Hagg et al., 2008) because more incoming shortwave radiation is absorbed in relation to the albedo reduction. This effect is canceled out by the thickening of the debris layer beyond this threshold: its low thermal conductivity induces an exponential reduction of the ablation rate. Thus, the development of decimeters to meters thick debris cover constitutes one of the most efficient negative feedback to current climatic changes, while worldwide glacier shrinkage is expected over the next decades (e.g., Huss and Hock, 2015).

This insulating layer confers specific behavior to heavily debris-covered glaciers. Because ice melt is limited in the ablation area, they have smaller accumulation area ratios than other glaciers (typically 0.1–0.4 instead of 0.6–0.7; Clark et al., 1994). They can thus have a positive mass balance with a restricted accumulation area, reach lower elevation and advance when neighboring bare-ice glaciers are retreating (Scherler et al., 2011; Deline et al., 2012; Carturan et al., 2013). The increase of debris thickness toward the glacier front can also reverse the ablation gradient, which usually induces a glacier surface flattening and limits the driving stress (Kirkbride and Warren, 1999; Benn et al., 2012). Thickness variations then become more pronounced than length variations for debris-covered tongues (Benn et al., 2003; Mayer et al., 2006). Finally, glacial hydrology and especially the concentration and the temporal variation of water release are also atypical in these systems (Mattson, 2000; Hagg et al., 2008). In this way, from a consequence of glacial dynamics, the covering of a glacier by a thick debris layer can become its main control (Deline et al., 2012).

Two main causes, enhanced by the acceleration of ice melt since the mid-1980s (e.g., Zemp et al., 2015), explain the current extent and thickening of supraglacial debris cover observed in mountainous regions (Kirkbride and Deline, 2013). Firstly, the deglaciation of rockwalls and permafrost degradation increase the debris supply to glacier systems (Bosson et al., 2015; Deline et al., 2015). Secondly, because the driving stress is positively related to ice thickness, thinning glaciers have weaker flow and, therefore, less ability to evacuate the sediment load to the hydrosystem (Benn et al., 2003; Paul et al., 2007). These two dynamics are particularly effective in the very small cirque glacier systems located in permafrost environments (Brazier et al., 1998; Seppi et al., 2015). Indeed, large amounts of debris are usually associated with these systems because of the rapid weathering of the surrounding rockwalls. Moreover, the height and surface of the latter can be lopsided in comparison with the restricted glacier surface (Maisch et al., 1999; Grunewald and Scheithauer, 2010). Finally, the debris evacuation can be limited because the weak driving stress of these thin ice masses is commonly reduced by the presence of cold ice (Gilbert et al., 2012) and/or large and possibly frozen sediment accumulations in the distal zone, such as moraine dam (*sensu* Benn et al., 2003), ice-cored moraines or rock glaciers (Shroder et al., 2000; Kirkbride and Deline, 2013; Bosson et al., 2015).

This contribution focuses on very small cirque debris-covered glacier systems located in permafrost environments. These particular systems are composed of a flowing ice mass mainly formed by the metamorphosis of snow (WGMS, 2008; Cogley et al., 2011; Dobhal, 2011), and associated, possibly frozen, debris accumulations. The existence of this type of glacier is especially related to the influence of the surrounding relief upon snow accumulation and shadow effects (Paasche, 2011; Capt et al., 2016). The size class of glaciers remains an open question in glaciology but 0.01–0.5 km^2 appear suitable thresholds to define very small glaciers (e.g., Kuhn, 1995; Fischer et al., 2014; Pfeffer et al., 2014). The ablation areas of the glaciers present in these systems are partly, or totally, debris-covered (Kirkbride, 2011). In the system margins, rock glaciers can be present. They are related to the long-term slow viscous creep of ice/debris mixtures under permafrost conditions, which generates particular surface patterns like ridges and furrows and a fine-grained steep front (Benn et al., 2003; Berthling, 2011; Monnier and Kinnard, 2015). In contrast to the debris-covered glaciers, they do not have accumulation areas from a glaciological point of view. The ice present below the block surface can have glacial (sedimentary ice) and/or non-glacial (e.g., magmatic ice) origin and its concentration is typically lower than within upslope glacier zones (usually <70%, e.g., Haeberli et al., 2006; Janke et al., 2015).

The landsystems investigated here remain poorly known in comparison with other glacier systems despite their large number and the fact that they can constitute considerable water reservoirs at a local scale (Azócar and Brenning, 2010; Knight and Harrison, 2014; Rangecroft et al., 2015). The complexity of these associations of ice and debris, their position at the frontier between glaciological and periglacial research and the confusion between debris-covered glaciers and rock glaciers mainly explain their limited consideration in cryospheric sciences (Haeberli, 2005; Berthling et al., 2013; Janke et al., 2015). Consequently, very small debris-covered glaciers associated with rock glaciers are commonly ignored in regional glacier inventories (Pfeffer et al., 2014). To our knowledge, no modeling considers their evolution. Furthermore, recent contributions investigated the transition from very small debris-covered glaciers to rock glaciers at the site-specific scale (e.g., Bosson et al., 2015; Emmer et al., 2015; Monnier and Kinnard, 2015; Seppi et al., 2015), but quantitative data on internal structure and on the operating processes are still lacking. In particular, the definition of the distinct components of these systems, the understanding of their origin and the identification of their responses to climatic variations is needed. This is the overall aim of this paper, which we achieve through the comprehensive study of three very small debris-covered glacier systems. The following research questions were addressed: what is the internal structure of these systems? How do their different components react to annual and seasonal climatic variations? What are the main processes involved in these responses?

STUDY SITES

Les Rognes, Tsarmine and Entre la Reille, the three sites investigated, are very small cirque glacier systems located in the north-western European Alps (**Figures 1**, **2**). In the three sites, the general concave topography between perched historic moraine accumulations show the glaciers shrinkage since the Little Ice Age (LIA). Ice outcrops are rare and the extensive debris cover masks the glacier limits. Meltwater streams are absent at the glacier outlet. Although water fluxes are visible and/or audible in summer, they disappear into the distal sediment bodies, emerging in temporary springs several hundred meters downslope. At the Holocene timescale, the high amount of sediment in the three systems contributed to the construction of imposing marginal sediment accumulations, part of which present typical rock glacier morphology. Because of these debris accumulations, the low slope angle, the weak glacial dynamics and the reduced meltwater streams, sediment evacuation is negligible. These systems are thus sediment sinks, decoupled from downslope

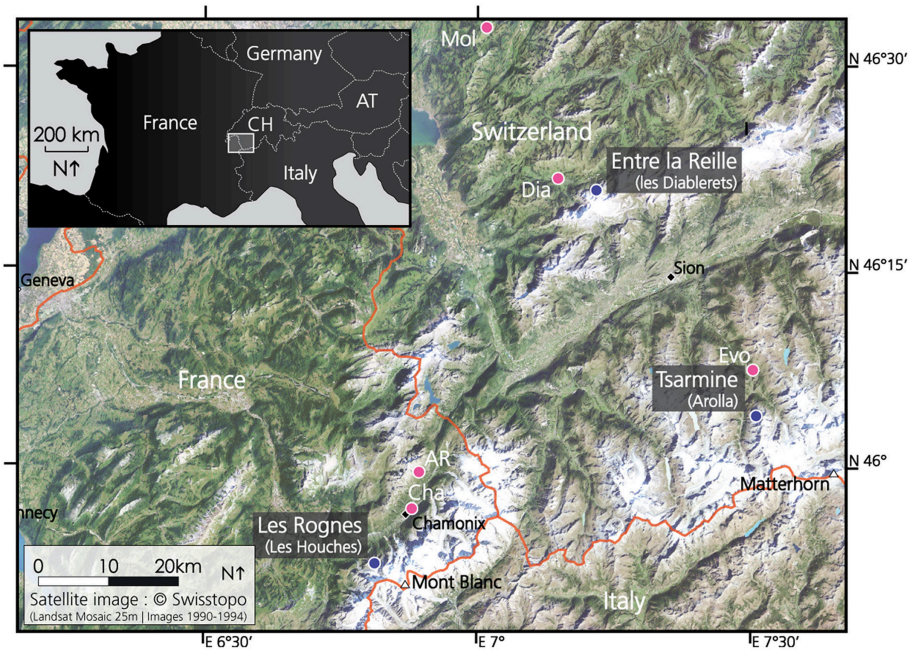

FIGURE 1 | Satellite image of the northwestern Alps showing the location of the three glacier systems studied. The red dots refer to weather stations.

sediment transfer systems (Shroder et al., 2000; Benn et al., 2003; Bosson et al., 2015). The investigated sites are located within permafrost areas, as shown by regional permafrost maps (BAFU, 2005; Bodin et al., 2008; Lambiel et al., 2009; Boeckli et al., 2012). The local occurrence of permafrost conditions was also shown in talus rock glaciers near les Rognes (Bosson et al., 2015; **Figure 2**) and Tsarmine (Lambiel et al., 2004; Micheletti et al., 2015), or in frozen talus slopes near Entre la Reille (Reynard et al., 1999).

Les Rognes Glacier System

Les Rognes (45°51′40″N, 6°48′50″E; 0.29 km^2; 2650–3100 m a.s.l.) occupies a small cirque oriented N-NW in the Mont-Blanc massif. The lithology is dominated by micaschists and gneiss (Mennessier et al., 1976). Mean annual air temperature is −1°C at 2800 m a.s.l. and annual precipitation is *c.* 2000 mm, according to Météo-France data (Chamonix and les Aiguilles-Rouges weather stations, respectively at 1042 and 2330 m a.s.l., **Figure 1**). The local equilibrium line altitude (ELA) has fluctuated above the glacier, at around 3200 m a.s.l. since the 1990s (Gilbert et al., 2012). This glacier is identified in the French glacier inventory and inherited from the disintegration of the LIA Tête-Rousse-Griaz-Rognes glacier complex (Gardent et al., 2014; Bosson et al., 2015). Today, under a 100 m high backwall, a debris-covered slope with few ice outcrops dominates a depressed area with marginal, rounded sediment ridges, which is terminated by a 30 m high steep slope in the northwestern part (**Figure 2**).

Tsarmine Glacier System

Tsarmine (46°03′N, 7°31′E; 0.49 km^2; 2600–3070 m a.s.l.) is located in the Pennine Alps. The bedrock is composed of granitic gneiss. Mean annual air temperature and precipitation are around −1°C and 1200 mm/yr at 2800 m a.s.l. respectively, according to MeteoSwiss data (Evolène weather station, 1825 m a.s.l., **Figure 1**). The Tsarmine glacier is identified in the Swiss glacier inventory (Fischer et al., 2014). The decadal mass balance variations and current geometry of this 4 × 10^6 m^3 ice mass are presented in Capt et al. (2016). These results exhibit its atypical behavior over time (mass balance divergence since the 2000s) and space (reversed ablation pattern) in comparison with other local glaciers, due to the combined influence of the decimeters thick debris cover, permafrost conditions, avalanching and solar shading on this very small glacier. Until the early 1980s, the upper part of Tsarmine glacier occupied the steep 600 m high north face of the Blanche de Perroc (Delaloye, 2008). The rockwalls are now deglaciated, providing an important sediment supply to the glacier. Shaded and crevassed debris-free glacier occupies the backwall foot. Arcuate rounded ridges are visible on the central part of the debris-covered glacier (**Figure 2**). The distal southern part, confined by the 100 m high moraine dam, is composed of glacier ice and ice-free debris (Lambiel et al., 2004). A lake of fluctuating level is also present since the 1980s. In the narrow northern distal part of the system, a rock glacier with a 15 m high steep front is present.

Entre la Reille Glacier System

Entre la Reille (46°20′20″N, 7°13′12″E; 0.04 km^2; 2380–2550 m a.s.l.) lies in the Diablerets massif where the lithology alternates limestone and marl (Badoux and Gabus, 1991). Mean annual air temperature and precipitation are respectively close to 0.3°C and 2000 mm/yr at 2450 m a.s.l., according to MeteoSwiss data (les Diablerets, and le Moléson weather stations, respectively at 1162 and 1972 m a.s.l., **Figure 1**). This ice mass has developed

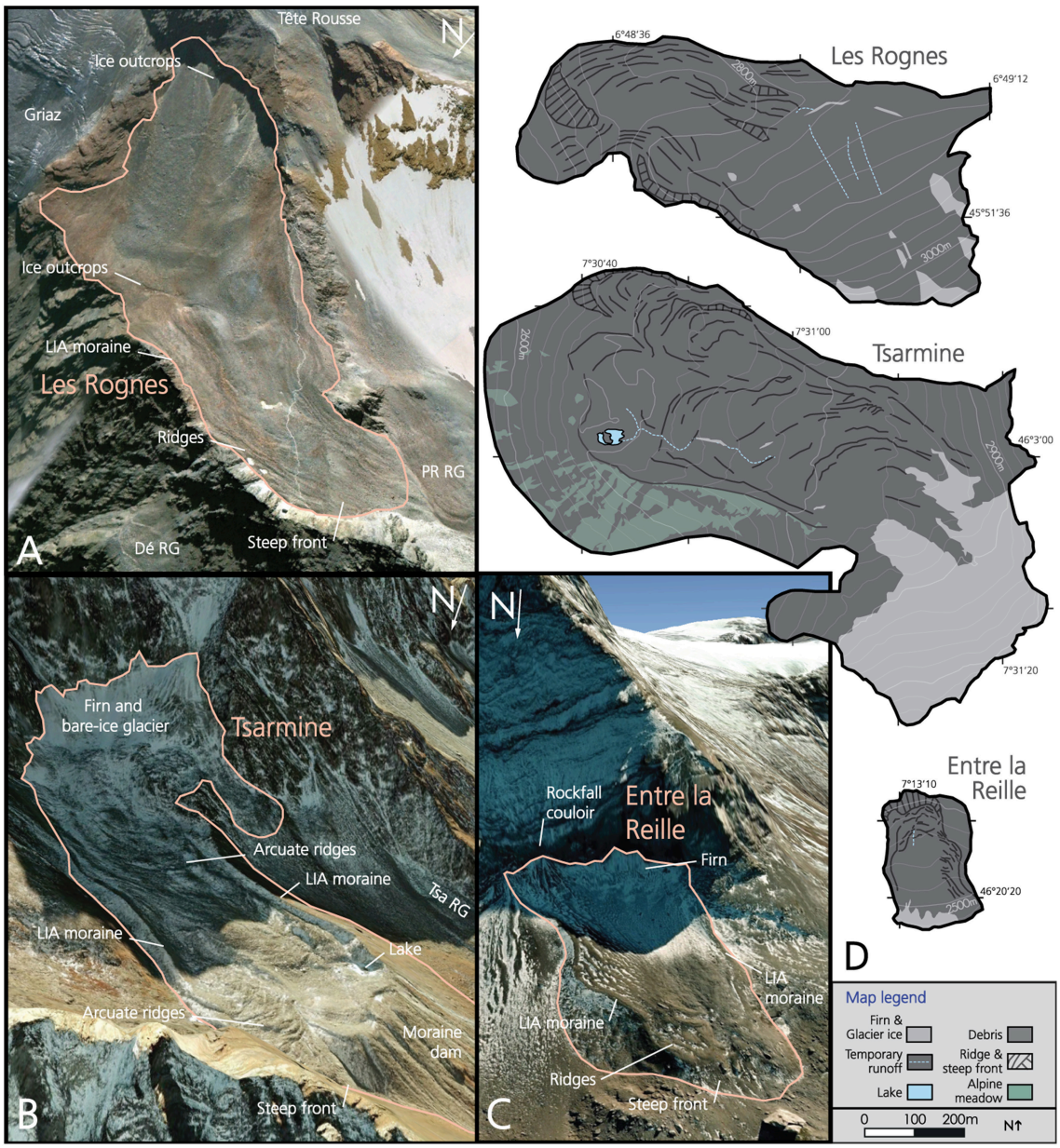

FIGURE 2 | 3D views of the study sites (A–C; © Google Earth 2015) and simplified maps (D). As the extension of glacier ice outcrops varies each year, its representation on map is an indication, derived from field observations and recent aerial images. RG refers to rock glacier in **(A)** and **(B)**.

below the 300 m high north face of the Oldenhorn. Previous geoelectrical surveys interpreted Entre la Reille as a body of sedimentary ice with locally high debris concentration, illustrating the burying of a very small glacier after the LIA (Reynard et al., 1999). In the upper zone, the concave west side contrasts with the convex east side, which is actively fed by a rockfall couloir (**Figure 2**). Ice outcrops are very rare and a small permanent snowfield occupies the top part. A gully where water can be heard in summer is present in the center. Ridges and furrows cover the distal part, which is delimited by a 20 m high steep fine-grained slope.

METHODS

General Approach

The internal structure and the current dynamical responses to short-term climatic variations were respectively assessed in the three study sites with Electrical Resistivity Tomography (ERT) and dGPS. In addition, current and recent surface morphology was analyzed with field observations, old oblique photographs that we collected, and numerous maps and aerial photographs available from the websites of national topographic institutes (map.geo.admin.ch and geoportail.gouv.fr; e.g., **Figure 3**).

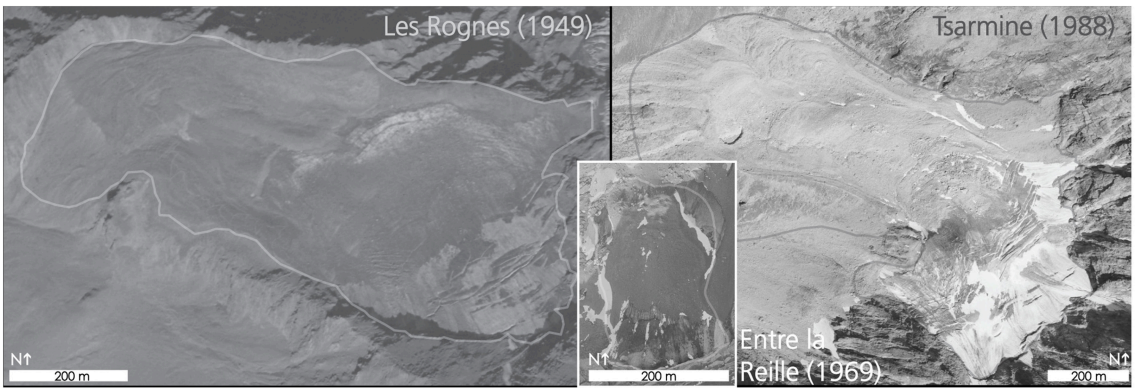

FIGURE 3 | Aerial images of the study sites. The Rognes picture was taken on 04/09/1949 (© IGN; n°IGNF_PVA_1-0__1949-09-04__C3630-0121_1949_F3630-3631_0045, available at geoportail.gouv.fr). The Entre la Reille picture (white inset) was taken on 29/09/1969 (© Swisstopo; n°19690475128861, available at map.lubis.admin.ch). The Tsarmine picture was taken on 10/08/1988 (© Swisstopo; n°19880990037583, available at map.lubis.admin.ch).

TABLE 1 | Date of dGPS surveys in each study site.

Study site	Early-summer surveys	Middle-summer surveys	Late-summer surveys
Les Rognes	19.07.2012; 22.07.2013; 18.07.2014	28.08.2012	05.09.2011; 03.10.2012; 26.09.2013; 26.09.2014
Tsarmine	10.07.2012; 08.07.2013; 24.07.2014	18.08.2014	13.09.2011; 25.09.2012; 08.10.2013; 23.09.2014
Entre la Reille	24.07.2012; 25.07.2013; 17.07.2014	22.08.2014	25.09.2011; 21.09.2012; 23.09.2013; 03.10.2014

However, we considered surface morphology with care because confusion and controversy emerged from morphology-centered approaches and relatively hampered the knowledge construction on the complex landsystems study here (Berthling, 2011; Janke et al., 2015). To simplify the analysis, we tried to identify homogeneous sectors that share the same general ground electrical resistivities, surface dynamics and morphology in each study site. We manually delineated them and concentrated on sectors where a large proportion of ice and debris are associated. Indeed, no direct measurements were possible on firn and bare ice zones because of rockfall hazards, and the weak surface activity of ice-free debris prevents to clearly distinguish movements from measure uncertainty.

Electrical Resistivity Tomography (ERT)

ERT was used because of its efficiency for ground ice characterization (Hauck and Kneisel, 2008). Indeed, the contrast between resistive ice and conductive unfrozen terrain allows the distinction between deglaciated debris (resistivity $r < 80$ kΩm), ice-debris mixtures ($5 < r < 1000$ kΩm) and massive sedimentary ice ($r > 500$ kΩm). These rough thresholds have to be considered carefully. They give an order of resistivity magnitudes, which also vary as a function of several factors (air/water content, temperature, etc.; Hauck and Kneisel, 2008). A scale of typical resistivities of material existing in permafrost environments is available in Bosson et al. (2015).

Profiles with 24 or 48 electrodes, sometimes overlapping, were measured at each site between summers 2011 and 2014. Ground apparent resistivity was measured with a Syscal Pro Swich 96 and a Junior Swich 48 (Iris Instruments, France). We used the Wenner-Schlumberger configuration because it constitutes a compromise between horizontal resolution and depth of investigation. The inter-electrode spacing was 5 m in the largest sites (les Rognes and Tsarmine) and 4 m in Entre la Reille. Following Hauck et al. (2003), salt-water saturated sponges were used to improve the electrical contact between electrodes and the porous surface material. Results were processed with Prosys II. To create a plausible image of the ground specific resistivities, data were inverted in Res2DInv with Least Square Inversions and Robust parameters (see details in Bosson et al., 2015). It allowed a good visualization of the high resistivity contrasts expected in these environments. The absolute error of the final tomograms is the difference between the inverted model and the measured data. The reliability of the inverted model was also evaluated by the model resolution matrix value (Hilbich et al., 2009). This method allows the areas near the surface where the model is well constrained by data (highest model resolution matrix values) to be distinguished from inversion artifacts (lowest values). 0.05 and 0.005 model resolution matrix values thresholds are displayed.

Differential GPS (dGPS)

The position of numerous blocks (87 in les Rognes, 78 in Tsarmine and 44 in Entre la Reille) was measured with a Leica SR500 or a Trimble R10 eight times between late September 2011 and 2014 (**Table 1**). These dGPS have respectively a theoretical maximum 3D accuracy of 0.05 and 0.02 m. The systematic measurement of control points showed that the accuracy was lower than 0.02–0.03 m. We considered movement values higher

than this threshold as significative. Field surveys were carried out in mid-July and late September to distinguish movements of the winter period with snow cover from those of the short snow-free period. Measurements were also performed in late August 2012 (les Rognes) and 2014 (Entre la Reille and Tsarmine) to compare the dynamics of early and late summer. However, the ablation period starts with the melt of the snow cover in spring. It can induce a glacier acceleration (e.g., Anderson et al., 2004). Unfortunately, because of the extensive thick snow mantle, it was not possible to measure the block positions in spring and the likely acceleration of velocities in the early ablation season is concealed in winter values.

As the mean slope angle around each block was not measured on site, it was derived from high-resolution digital elevation models (DEMs): 4 m resolution at les Rognes (source: RGD 73–74) and 2 m resolution at Entre la Reille and Tsarmine (source: Swisstopo). The mean standard deviation of the slope angle calculated in a 12 m square around each block was lower than 3°. Assuming no change in surface gradient between surveys, we computed the values of expected vertical movements ($dZ_{exp.}$) and downslope movements (M_d) from horizontal movements (dX) and the slope angle for each block (**Figure 4**). dH, namely the difference between $dZ_{exp.}$ and dZ, was then derived (see Isaksen et al., 2000, for similar methodology). This value provided useful indication of local topographical variations, related to ice volume variation and/or compressing/extending flow. We assess the uncertainty of dH by calculating the means of dX, dZ and slope angle for all the blocks of each site. Then we recomputed dH taking into account these means and their respective uncertainty values. The standard deviation of the dH obtained was around 0.05 m.

Indices were computed by homogeneous sector in each system to characterize the intensity, the temporal variation and the type of the occurring dynamics. We used the blocks whose positions were measured in every field survey for this calculation. Here, we only present the mean of the values obtained in the three systems. Indeed, the same contrasted dynamical behaviors between the system components appeared clearly in each study site. The calculated mean indices provide, therefore, indications of the dynamical behaviors that can be found in these landsystems. To assess the sensitivity to short-term and medium-term climatic variations, we calculated the standard deviation of seasonal and annual velocities of every individual year for each sector. In addition, the proportions of movement for each season and each part of summer were computed to highlight the main periods of activity. We also calculated the downslope movement/surface lowering (M_d/dH) ratio to determine which dynamic is dominant: the downslope movement value is higher than the surface lowering one when $M_d/dH > 0$, equal when $M_d/dH = 0$ and smaller when $M_d/dH < 0$. Finally, following Copland et al. (2009) and using the mean horizontal velocities between 2011 and 2014, three Velocity Cross-Profiles (VCP) for each study site were used to highlight the dominant motion mechanism. Cubic-shaped velocity cross-profiles suggest an en masse movement related to the basal sliding. Conversely, a parabolic shape indicates the internal deformation of viscous fluid, related to the friction increase toward the margins (Cuffey and Paterson, 2010). This method was used for larger glaciers and has to be considered with caution here because the horizontal velocities taken in account have weak magnitude. However, the results obtained here and at the decadal timescale (see Capt, 2015) illustrate that analysis of velocity cross-profiles also provides valuable information on the motion mechanisms in very small glacier systems.

RESULTS

ERT Results

In the Rognes glacier system, resistivity values are very high (>1000 kΩm) directly under the surface of the 250 m long upper

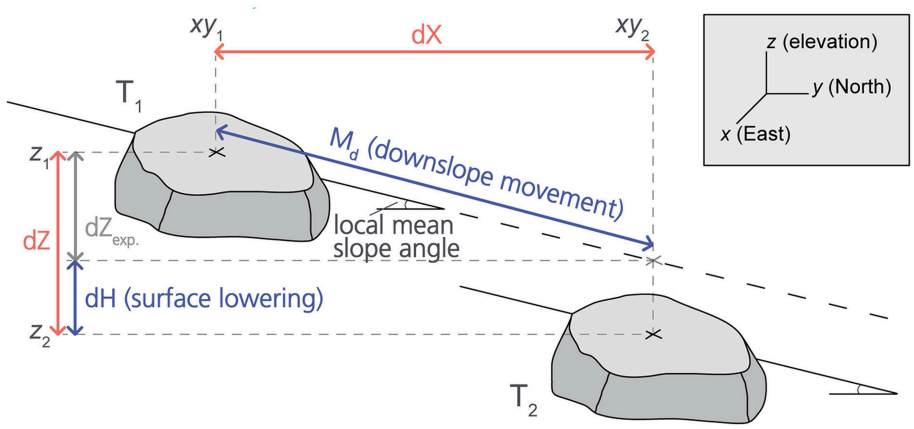

FIGURE 4 | Sketch showing the principle of a dGPS measurement and the parameters that can be calculated with a moving block: dX (*horizontal movement*), dZ (*vertical movement*) and, if the slope angle has not significantly varied during the two measurements, M_d (*downslope movement*, derived from dX and the local mean slope angle), $dZ_{exp.}$ (*expected vertical movement* derived from dX and the local mean slope angle) and dH (the difference between expected movement and the measured vertical movement; this parameter is an expression of surface lowering).

slopes of Ro-2 (**Figure 5**). The thickness of this structure is hard to define, because the inversion is poorly constrained by the data at depth (very low model resolution matrix values). A 200 m long conductive zone showing resistivities mostly lower than 10 kΩm, occupies the flatter downslope area. The end of Ro-2 and Ro-1 cross ridges and furrows in a 250 m long convex zone toward the NW, contrasting with the previous concave zone. Resistivities reach 500 kΩm under 3–5 m of conductive material (<30 kΩm), in a structure where model resolution matrix values are very low. The values decrease to 5–50 kΩm in the 80 m located above the north steep fine-grained front (Ro-1). Finally, the south part of the cross-profile that cuts the distal zone (Ro-A) shows a 100 m large and approximately 25 m thick highly resistive structure (>500 kΩm) under several meters of conductive material. This contrasts with moderate resistivities in the north (<150 kΩm).

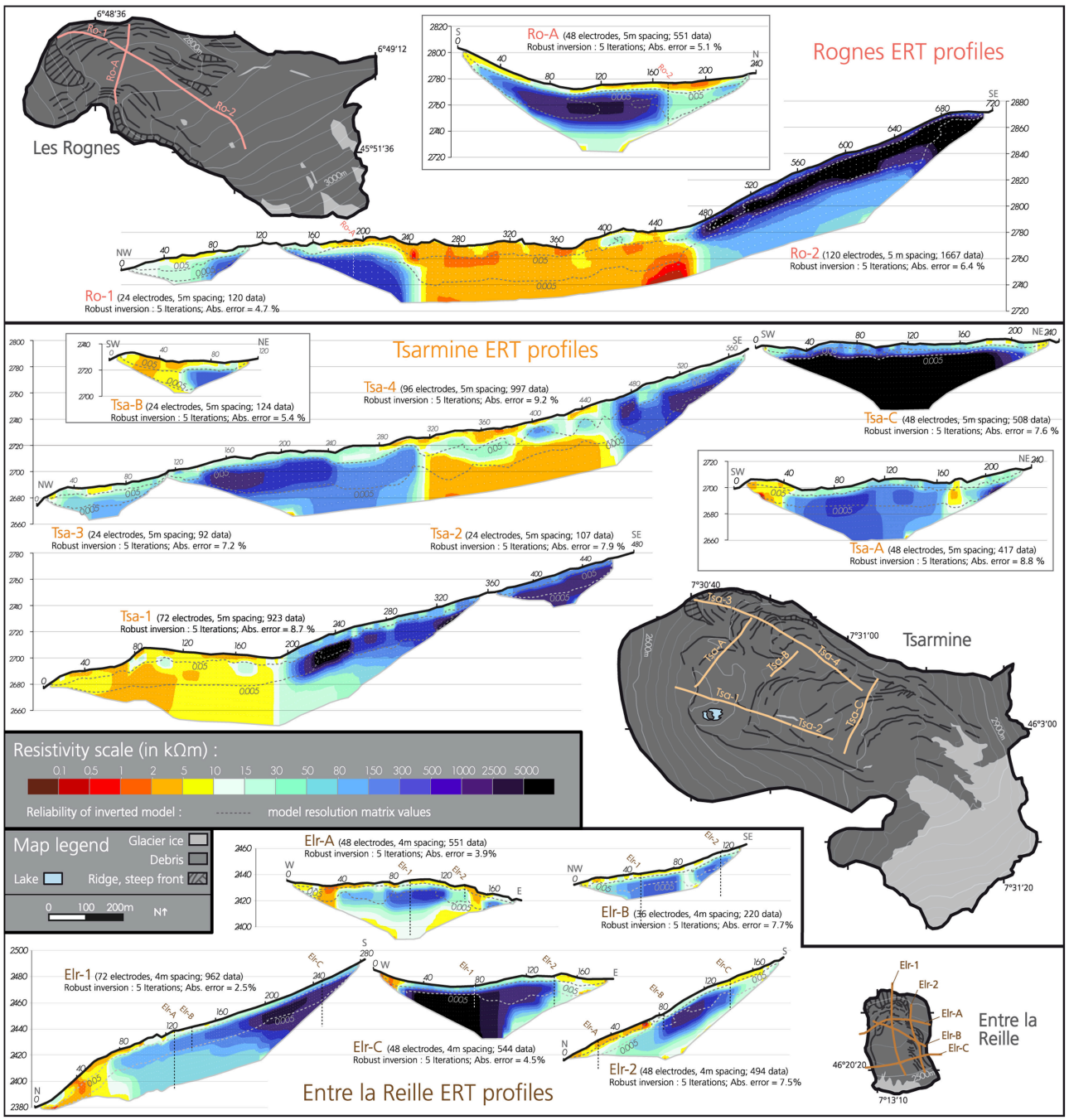

FIGURE 5 | Longitudinal (1, 2, 3, and 4) and transversal (A, B, and C) electrical resistivity tomograms (ERT) profiles obtained in August 2012 at les Rognes, in August 2014 at Tsarmine and between 2011 and 2013 at Entre la Reille.

In Tsarmine, resistivities exceed 5000 kΩm at a depth of 4–6 m over the whole width of the upper zone (Tsa-C). The prolongation of this structure is observable downslope (120 m long in the SE of Tsa-4 and 250 m long in Tsa-2 and in the SE of Tsa-1) but the resistivity values drop locally to 150 kΩm. A 150 m long more conductive zone with patchy resistive structures ($2 < r < 300$ kΩm, 15 m thick, center of Tsa-4) occupies the slope located above the distal 300 m long rock glacier-like sector. In this zone (NW of Tsa-4 and Tsa-3), resistivities can exceed 1000 kΩm under several meters of material with higher conductivity (<30 kΩm). Tsa-B shows contrasted resistivities and Tsa-A illustrates the presence of a resistive structure (>150 kΩm) a few meters below the surface of the flakt distal area. Finally, a conductive zone (<30 kΩm; NW of Tsa-1 and SW of Tsa-A) composes the southwestern margin near the lake.

The upper part of Entre la Reille contains a very resistive layer located close to the surface in the west concave part (>1000 kΩm on Elr-1 and Elr-C). A 50 m long resistive layer (>150 kΩm; Elr-2 and SE of Elr-B) composes the east convex side, where surface deformation patterns are visible. Its thickness is around 20 m, but here the model resolution matrix values are low. The resistivities progressively drop toward the distal part and values become lower than 10 kΩm in the steep fine-grained front (Elr-1). Finally, a layer of moderate to high resistivities (<1000 kΩm; Elr-A and Elr-B) is visible in the central zone below several meters of material with high conductivity.

dGPS Results

For each block, we calculated the total, yearly, seasonal and early/late summer horizontal (v_x), vertical (v_z) and surface lowering (v_h) velocities. Only the mean velocities (v) for the whole period are presented here to give an overview (**Figure 6A**).

All the blocks in the Rognes system moved more than 0.02 m yr^{-1} between 2011 and 2014. The most significant velocities occur in the upper slope, with all component values being higher than |0.25| m yr^{-1}. Here, surface lowering is smaller than −0.5 m yr^{-1} for many blocks. Downslope, most of the blocks are moving toward the central depression with moderate velocities ($v < |0.25|$ m yr^{-1}). The distal part is generally flowing toward the west and SW. v_x values sometimes exceed 0.5 m yr^{-1} whereas the v_z and v_h values are smaller (−0.05 to −0.25 m yr^{-1}) on the south part of the front than on the north.

In Tsarmine, the most striking behavior concerns the blocks situated in the upper zone, corresponding roughly to half of the blocks. Movements are homogeneous: v_x values toward the NW are faster than 0.5 m yr^{-1}, whereas v_z values range between −0.25 and −1 m yr^{-1}. The highest surface lowering ($v_h < -0.25$ m yr^{-1}) is observed here and in a small zone in the center of the distal part. Elsewhere, velocities are more variable. On the rock glacier, velocities are mainly significant in the horizontal component ($v_x > 0.1$ m yr^{-1}) and surface lowering is weak. The south frontal part experiences very slow multidirectional movements.

Entre la Reille is a completely active system, although velocities never exceed |0.5| m yr^{-1}. v_x, v_z and v_h values range mostly between |0.1| and |0.25| m yr^{-1} in the top and central part, corresponding to almost two thirds of the blocks. The margins show similar to smaller v_x and v_z values, but the surface lowering rate is weaker. The four blocks located on the steep fine-grained front reflect a slow horizontal north oriented flow ($v_x < 0.1$ m yr^{-1}).

System Components

ERT and dGPS results, field observations and historical documents provide coherent information on the system components. For example, the net changes in homogeneous surface kinematic behaviors between the top slopes and the distal flat zones in les Rognes or Tsarmine (**Figure 6A**) precisely correspond to large contrasts of ground resistivity (Ro-2 and Tsa-1 in **Figure 5**). The differences of resistivities also match spatially with differences in surface characteristics, such as the presence of ridges and ice outcrops, visible during the field campaign or on historical images. Another example is the upper zone of Entre la Reille. The concave left-hand side and the convex right-hand side, where superficial deformation patterns are numerous, clearly exhibit distinct ground resistivities. With all these consistent elements, five main homogeneous sectors can be defined, characterized (**Tables 2, 3**) and mapped (**Figure 6B**) in each site.

Firn and bare-ice glacier zones occupy variable parts of the top of the glacier systems, changing each year in relation to the snow accumulation at the end of the melt season and the spread of the debris mantle. A thin (millimeters to decimeters) and discontinuous debris layer can cover the snow and ice. Buried ice is also exposed locally by supraglacial landslides and by incision related to water runoffs in the debris-covered zones. Currently, this sector is continuous and occupies a large area (0.11 km^2; **Table 3**) at Tsarmine. Here, avalanches enhance the snow accumulation. Its metamorphosis in ice and downward flow is illustrated by the presence of crevasses (**Figures 2**, **3**). In les Rognes, the size of this zone, where crevasses and bergschrund were visible in last decades (**Figure 3**), is now very restricted. Conversely, the upper zone of Entre la Reille has been occupied only by a firn area whose extension has changed continuously over the last decades.

Debris-covered glacier zones are present in large portions of the systems (**Table 3**), generally in the top and central concave parts (**Figure 6B**). They illustrate the progressive covering of the glaciers since the LIA. Crevasses are observable in these sectors on aerial images of les Rognes and Tsarmine until the early 2000's (**Figure 3**). These zones may also have been temporarily covered by snow at the end of the ablation seasons over the last decades but this situation has become rare since the 1980's. The high measured resistivities (>500 kΩm, with extended zones >5000 kΩm) reveal that these sectors are composed of massive sedimentary ice with probably low debris content. The current thickness of the glaciers is unknown, except in Tsarmine where a GPR survey in 2015 revealed respectively mean and maximum thickness of 15 and 35 m (Capt et al., 2016). According to its dimension and the height of the surrounding moraines, this glacier is likely the thickest of the three studied here. Supraglacial debris thickness can vary locally but generally increases downglacier (decimeters to meters

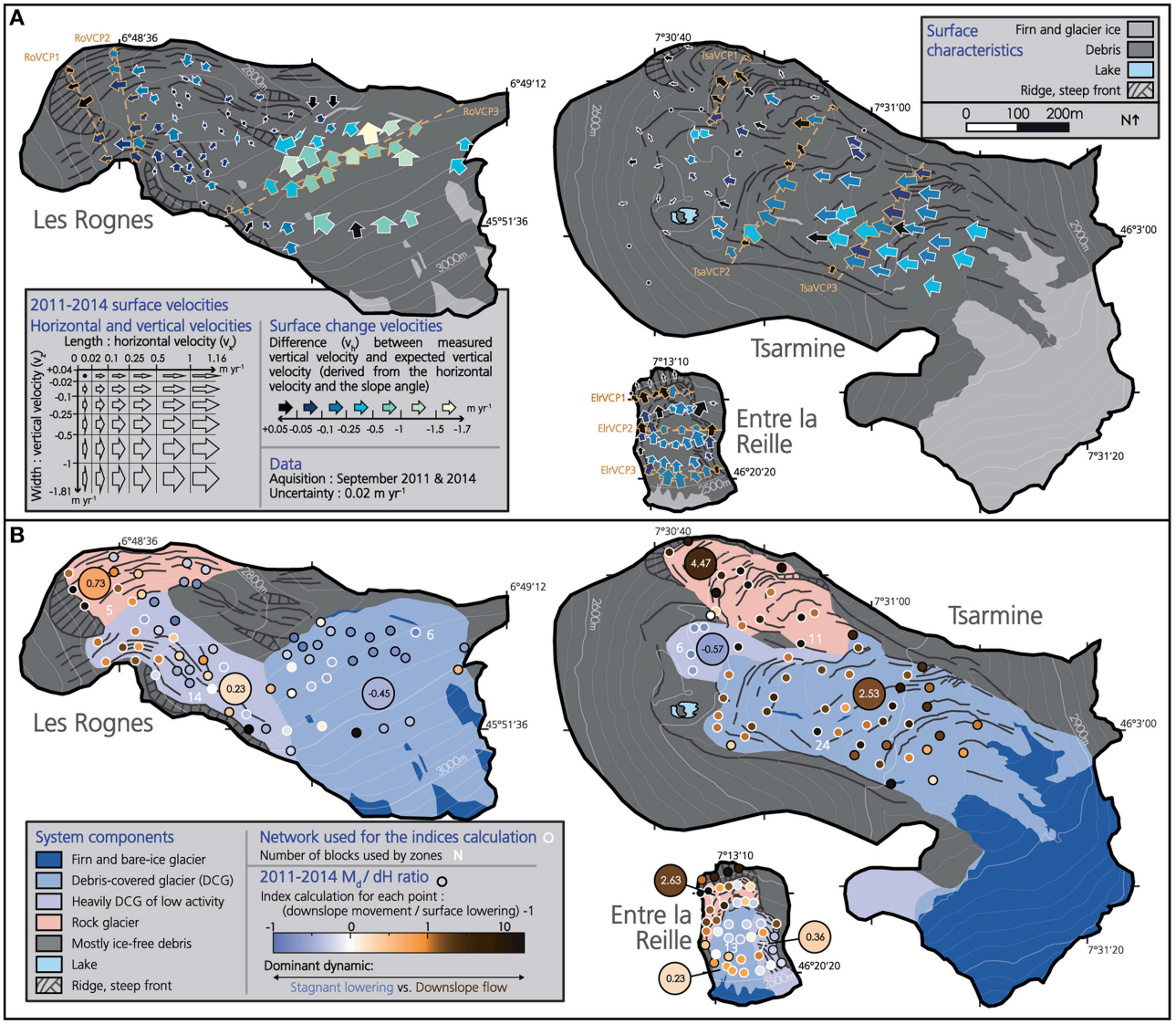

FIGURE 6 | (A) Velocities measured with dGPS in the study sites between September 2011 and 2014. Orange lines correspond to the velocity cross-profiles of **Figure 8** where the horizontal velocity of the points in orange is depicted. **(B)** Components of the glacier systems and downslope movement/surface lowering (M_d/dH) ratio results based on the movements measured between September 2011 and 2014 **(A)**. The large circles correspond to the mean M_d/mean dH value by zone in each site. White circles correspond to the position of the dGPS network used for the calculation of the dynamical index in **Figure 7**.

according to ERT results and field observations). The surface topography is undifferentiated, except in Tsarmine, where many arcuate rounded ridges are present. They were generated by the compressive stress induced during the downward migration of the snow and ice accumulated in the 1960s to mid-1980s period (Capt et al., 2016). Water runoff is observable or audible in summer especially in gullies (**Figure 2**). In each site, the fastest surface velocities were measured in these zones.

Heavily debris-covered glacier zones of low activity are present in some marginal areas. It starts at the foot of the backwall on the east of Entre la Reille and prolong downslope from the debris covered glacier parts in les Rognes and Tsarmine. The transition between these two sectors is gradational, even though several characteristics allow their distinction. Heavily debris-covered zones are also composed of buried massive ice but the concentration of englacial debris is probably higher, as revealed by lower resistivities (80–2500 kΩm). Moreover, the surface layer where the resistivity decreases is thicker, suggesting that the supraglacial debris layer here reaches several meters. It explains the rare observations of ice outcrops and runoff. Surface velocities are weak, exceeding rarely |0.25| m yr^{-1}. The rounded ridges present in les Rognes and Entre la Reille probably result from the slow local viscous deformation. No crevasses or ice outcrops have been visible in these sectors over the last decades, illustrating the weak dynamic of these completely buried glacier zones (**Figure 3**).

TABLE 2 | Characteristics of the main components of these glacier systems.

Parts of the glacier system	Surface characteristics	Surface curvature	Massive ice outcrop	Water runoff in summer	Soil and vegetation	Debris cover (active layer) thickness	Ground resistivity	Surface velocity
Firn and bare-ice glacier	- Ice/snow surface varying between years - Locally covered by dust or debris - Crevasses (Tsa)	Concave (except avalanche cones in Tsa)	Everywhere	Visible and/or audible	Absent	Absent to few centimeters	Probably >1000 kΩm	Probably several decimeters to meters per year
Debris-covered glacier	- Mainly coarse debris - Relatively undifferentiated topography (except in Tsa) - Arcuate rounded ridges (on Tsa, ELR) - Angular crest on the side (Tsa and ELR) - Rare gullies	Mainly concave	Rare	Visible and/or audible	Absent	Decimeters to meters	>500 kΩm	Several decimeters to meters per year
Heavily debris-covered glacier of low activity	- Mainly coarse debris - Relatively differentiated topography - Angular crest on the side (Tsa and ELR) - Arcuate rounded ridges	Concave (Tsa) and convex (Ro, ELR)	Very rare	Rarely Visible and/or audible	Absent	Several meters	>100 kΩm	Centimeters to decimeters per year
Rock glacier	- Mainly coarse debris - Organized viscous, topography - Arcuate ridges and furrows - Distal steep fine-grained front	Mainly convex	Absent	Absent	Absent (except rare developments in Ro)	Several meters	>10 kΩm	Centimeters to decimeters per year
Mostly ice-fee debris	- Coarse and fine debris - Angular crests on the side and arcuate rounded ridges	Mainly concave	Absent	Absent	Absent (ELR) to various stage of development	Meters to several tens meters of deglatiated debris	>30 kΩm	Null to few centimeters per year

TABLE 3 | Area (in km^2) and mean slope angle (in degree) of the main components of these glacier systems.

	Les Rognes (area in km^2; mean slope in °)	Tsarmine	Entre la Reille	Mean
Firn and bare_ice glacier	0.01; 39	0.11; 29	0.003; 33	0.04; 34
Debris-covered glacier	0.13; 24	0.15; 18	0.013; 23	0.10; 22
Heavily debris-covered glacier of low activity	0.05; 20	0.03; 17	0.009; 29	0.03; 22
Rock glacier	0.03; 12	0.04; 18	0.007; 28	0.03; 19
Mostly ice-free debris	0.09; 24	0.17; 28	0.010; 33	0.12; 28
All	0.29; 24	0.49; 25	0.042; 28	0.27; 26

Rock glaciers occupy some frontal and lateral parts of the systems investigated. Again, the transition with the neighboring zones is gradational. ERT profiles exhibit generally lower resistivities than in the previous glacier zones. The moderate resistivities (10–150 kΩm) show the probable overall higher debris-concentration in the ground and the domination of ice-cemented structures. However, resistivities reach 2500 kΩm in some locations, illustrating the presence of massive ice lenses. No ice outcrops or evidence of water runoff were visible in these sectors during field investigations or in historical sources. The surface morphology, composed of arcuate ridges and furrows bounded by a steep fine-grained front, has not shown remarkable changes over the last decades (**Figures 2**, **3**). It illustrates the long term slow viscous deformation of frozen debris. Currently, slow sub-horizontal movements dominate and surface lowering is very low.

Ice-free debris zones are essentially present in the steep distal areas (**Table 3**). The low resistivity values (0.5–30 kΩm) show the generalized absence of ground ice. The debris thickness can reach several tens of meters. Patches of vegetation are present locally (**Figure 2**). In Tsarmine, a small lake developed in this sector in the 1980's (**Figure 3**). Surface movements are mainly lower than 0.1 m yr^{-1}.

Current Dynamics

The *intensity of dynamics* was investigated by the calculation of annual, summer and winter v_x, v_z, and v_h means (**Figure 7**). Debris-covered parts of the glaciers have the highest velocities in all periods. The annual v_x, v_z and v_h means ($<|0.5|$ m) are relatively homogeneous. In summer, v_x values are four times and v_z and v_h values more than 1 times faster than during winter. Mean velocities exceed 1 m yr^{-1} in summer and vertical and surface lowering values are especially high (< -1.6 m yr^{-1}). The latter are low in winter (> -0.14 m yr^{-1}), while v_x values remains relatively high at 0.28 m yr^{-1}. Seasonal variations are similar in heavily debris-covered glacier zones, although the overall velocity values are about three times lower. Annual velocities do not exceed $|0.2|$ m yr^{-1}, summer velocities are limited to $|0.67|$ m yr^{-1} and winter values are minor (especially v_h). The situation is different in rock glaciers, where maximal velocities reach $|0.25|$ m yr^{-1}. The v_x values are relatively constant during summer and winter. The main change concerns the summer acceleration and winter deceleration of v_z and v_h. On the annual timescale, the surface lowering is very weak (-0.04 m yr^{-1}).

The *temporal variation of dynamics* was assessed by computing the standard deviation of annual and seasonal velocities of all the individual years and quantifying the proportion of movement realized each season and each part of summer (**Figure 7**). Debris-covered glacier zones have the highest Standard deviation values, indicating a high temporal variability of velocities. Most of the annual movements occur in summer (almost the whole surface lowering), whereas early and late summer activity is balanced. On the other hand, marginal rock glaciers experience low temporal velocity variability (standard deviation <0.08) and generally winter dominant dynamics. Summer activity is mainly concentrated in late summer, especially in vertical and surface lowering components. Between these two opposing behaviors, heavily debris-covered glacier zones have moderate standard deviation values, summer and late summer dominant dynamics.

The *dominant dynamic* was evaluated by comparing downslope movement and surface lowering values (**Figures 6B**, **7**). Debris-covered glacier zones show the most heterogeneous M_d/dH values (**Figure 6B**). Indeed, values were negative here in les Rognes and in the lower part of Entre la Reille and positive in the upper part of the latter and in Tsarmine. The mean value of 0.77 in these three zones reflects the slight domination of downslope flow (**Figure 7**). M_d/dH values are also heterogeneous in heavily debris-covered glacier zones but the global mean suggests that downslope movement and surface lowering have similar magnitudes here. Finally, rather homogeneous values are found in rock glaciers, where M_d/dH is commonly above 1. The mean of 2.61 between these zones in the three sites illustrates the predominance of downslope flow.

The *motion mechanism* was inferred from 9 horizontal velocity cross-profiles (**Figure 8**). Appearances of the velocity cross-profiles do not reveal undisputable cubic or parabolic patterns, showing the probable multiple origin of motion. For example, TsaVCP3 gathers cubic and parabolic aspects: at least 0.5 m yr^{-1} can be attributed to an en masse movement that adds up to the central velocity increase related to internal deformation. On the left hand side of RoVCP1, RoVCP2, RoVCP3, TsaVCP2, ElrVCP3, on TsaVCP3 and on the right hand side of ElrVCP2, the rapid increase of velocity from the margin and/or the main tabular-shape of velocity profiles indicate the likely occurrence of basal sliding. Conversely, the profiles are arcuate and velocity progressively increases toward the central flowline in the northern side of RoVCP1, RoVCP2, TsaVCP2 and on TsaVCP1 and ElrVCP1, reflecting the effect of internal deformation. Thus, basal sliding seems important in (heavily) debris-covered zones whereas the rock glaciers appear mainly affected by internal deformation.

INTERPRETATION AND DISCUSSION

Internal Structure

Figure 9 synthetizes our interpretation of the internal structure of the main components encountered in the study sites. The

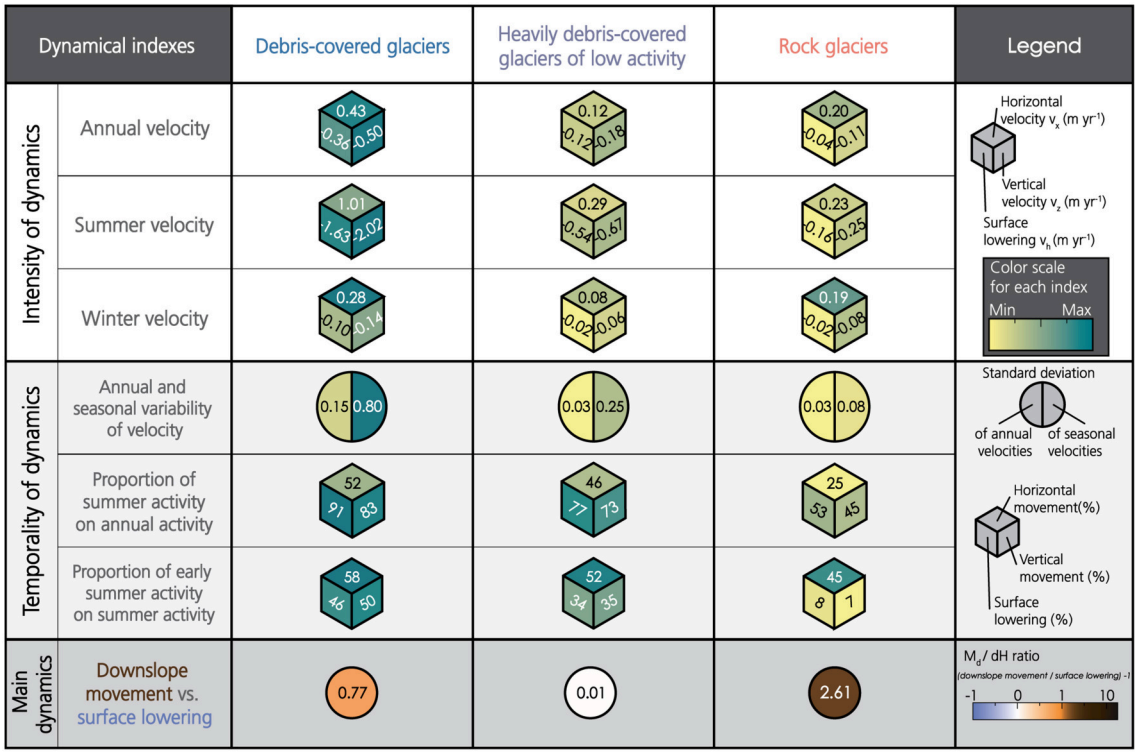

FIGURE 7 | Mean values of dynamical indexes calculated by zones where ice and debris are associated in the three study sites with dGPS data. The dGPS network used for this calculation appears in **Figure 6B**.

comprehensive results obtained are in line with the internal structure characteristics proposed in this type of landsystem by individual site studies (e.g., Kneisel, 2003; Reynard et al., 2003; Kneisel and Kääb, 2007; Ribolini et al., 2010; Monnier et al., 2014). At the system scale, atypical characteristics differentiate the study sites from the larger and bare-ice glacier stereotype: the small size of the upslope firn and bare-ice zones and the associated large relative area of debris-covered glacier zones, the existence of marginal rock glaciers and the overall very high amount of debris in comparison with the glacier size. The glacier zones are extensively covered by a coarse-grained debris layer that thickens downglacier due to flux emergence, compressive stress and ice melt (Kirkbride and Deline, 2013). This also explains the debris concentration increase in the glacier margins. These very small glaciers have, therefore, typical characteristics of buried glaciers (Ackert, 1998; Janke et al., 2015). In rock glaciers, large ranges of ground electrical resistivities were measured (**Figure 5**), outlining the coexistence of ice-cored and ice-cemented structures under the several meters thick unfrozen surface layer. The decrease of ice concentration and increase of surface debris layer thickness distinguish rock glaciers from debris-covered glaciers here, as proposed by Janke et al. (2015). Finally, ice-free debris areas are present in the frontal and some lateral zones of the studied systems.

Surface Movements and Associated Processes

Figure 9 also synthetizes the current responses to short-term climatic variations detected in the studied systems. Two main dynamics are active: (1) surface lowering, which can be related to ice melt and extending flows (Lambiel and Delaloye, 2004); and (2) downslope movement, which can result from internal deformation, basal sliding and bed deformation (Haeberli et al., 2006; Benn and Evans, 2010). Only ice melt, basal sliding and internal deformation are considered here, since we have no data on the possible bed deformation. Moreover, extending flows that occurs locally (**Figure 6A**) were not quantified as the thickness of the deforming bodies is largely unknown. However, ridges and furrows and surface velocities suggest the large domination of compression. We interpret, therefore, surface lowering (v_h) mainly as an expression of ice melt rather than extending flow. Its high value in stagnant zones or where compressive stress would compensate surface lowering (e.g., the footslope of the debris-covered zone of les Rognes) supports this interpretation. The dynamical behaviors of debris-covered glacier zones, heavily debris-covered glacier zones of low activity and rock glaciers are respectively discussed in the following paragraphs.

Polythermal glaciers are common in permafrost environments (Etzelmüller and Hagen, 2005; Gilbert et al., 2012). This situation

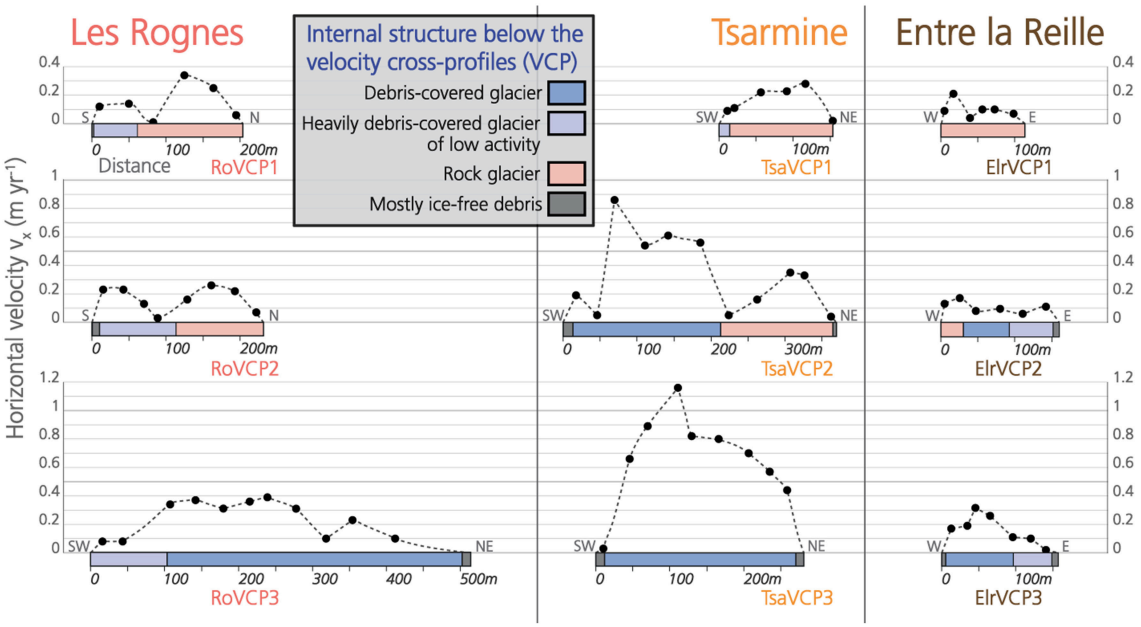

FIGURE 8 | Velocity cross-profiles (VCP) obtained from horizontal velocities between September 2011 and 2014 and internal structure below each profile. The 9 cross-profiles and the data used are depicted in **Figure 6A**.

may characterize the studied glaciers (Bosson et al., 2015). However, the proportion of cold ice seems low at the base of the debris-covered glacier zones if we consider, as other authors, basal sliding signature as an indicator of temperate ice (Mayer et al., 2006; Bingham et al., 2008; **Figure 8**). The basal sliding pattern also clearly appears at the decadal timescale at Tsarmine glacier (Capt et al., 2016). The influence of water here is likewise supported by the marked seasonal variation of surface velocities, the recording of maximum horizontal velocities in early summer when the water production is very high and field observations and audition of water circulation. Hence, these sectors, where an efficient drainage network can be present (Pourrier et al., 2014), show rapid responses to climatic and hydraulic forcing during the melt season. Our results suggest the following annual behavior. The snow cover strongly decouples the glacier from the atmosphere between October and June. Surface lowering is slight and horizontal movements produce half of the annual total (**Figure 7**). Winter motion is mainly attributed to internal deformation because basal sliding often deactivates (Anderson et al., 2004; Bingham et al., 2006). During summer, the ablation rate is very high and induces most of the annual surface lowering (91%). The water supply increases the flow. Mean v_x decreases in late summer, probably because of the drainage network development at the glacier bed (Anderson et al., 2004; Rippin et al., 2005; Bingham et al., 2006). The maximum movements are then observed in the zones where water runoffs are concentrated, as in the SW of Tsarmine (**Figure 2** and TsaVCP3 and TsaVCP2 of **Figure 8**).

The presence and influence of water is also possible in heavily debris-covered glacier zones, considering its summer observation and audition, the cubic shape of velocity cross-profiles (**Figure 8**) and the summer dominant activity (**Figure 7**). However, Evans (2013) suggested that viscous surface patterns, as observed in these sectors in les Rognes and Entre la Reille, illustrate a cold thermal regime and therefore low water content. Ice melt, basal sliding and ice deformation seem active here but with a weaker intensity than in debris-covered glacier zones (**Figure 7**). The period of activity is brought forward to late summer and winter because of the filtering of short-term climatic variations by the weakly thermally conductive thick debris cover.

The motion of rock glaciers appears mostly due to internal deformation. Water content and influence seem low: no water runoff was heard during field campaigns, velocity cross-profiles have a parabolic aspect, dynamics occur mainly in winter and mean v_x is relatively stable over the year (**Figure 7**). However, water can be temporarily present in rock glaciers and influence their dynamics (Haeberli et al., 2006; Hausmann et al., 2007; Delaloye et al., 2008). It could explain the slight increase in velocities observed in summer. Surface lowering is almost ineffective at the annual timescale, illustrating the low ice melt. Thus, only internal deformation seems noticeably effective here and short-term climatic variations induce attenuated and shifted responses. This behavior contrasts, therefore, with the one observed in the upper glacier zones. Its origin is mainly related to the filtering and slow propagation of summer temperatures in the poorly conductive thick superficial debris layer (Delaloye et al., 2008), the limited ice concentration, and if water is present, its probable slow and diffuse circulation (Pourrier et al., 2014).

In the studied systems, direct and high-magnitude responses contrast with delayed and attenuated responses to short-term climatic variations. This different climate sensitivity appears

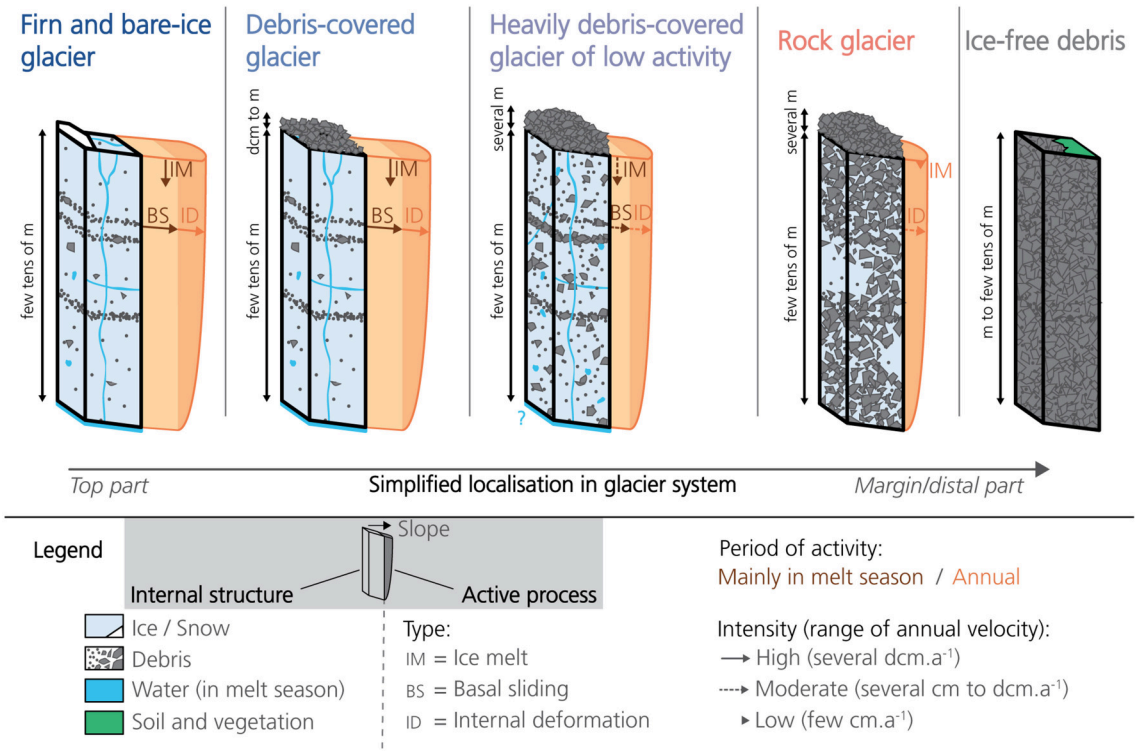

FIGURE 9 | Schematic diagrams showing the internal structure characteristics and the main dynamics occurring in the five main zones of les Rognes, Tsarmine and Entre la Reille systems.

mainly related to the proportion of ice, debris and water (and associated hydrological network properties) in the ground and the thickness of the superficial debris layers (**Figure 9**). This is in accordance with previous studies, which illustrated the influence of these factors individually: climate sensitivity in ice-debris associations decreases when the ice concentration reduces (Kääb et al., 1997), when the superficial debris layer thickness increases (Benn et al., 2003; Kirkbride and Deline, 2013), when the water content decreases (Schomacker and Kjær, 2007) and when the water circulations are null or rare and diffuse (Pourrier et al., 2014). Finally, null to very slow movements were measured in the ice-free debris zones, illustrating the strong control of ice content on surface dynamics (**Figure 6A**).

Genesis and Evolution

The genesis of the studied systems has to be considered in light of the numerous Holocene climatic oscillations, although their current structures are mainly related to the last glacial pulse (LIA and subsequent decay; Ackert, 1998; Matthews et al., 2014; Monnier et al., 2014). Indeed, the extent of both glacier and debris-covered zones probably continuously oscillated over the last millennia in relation to climatic variations (e.g., Ivy-Ochs et al., 2009). During positive mass balance periods, glaciers were larger than today and progressively accumulated lopsided amounts of sediments at their bed and margins. Their accumulation areas shrank and even disappeared under warmer and/or drier conditions, as it has occurred since the end of the LIA. Unable to evacuate the debris provided by the bed erosion and weathering of the backwalls, these very small rag glaciers progressively became stagnant, downwasting and buried ice bodies (Bosson et al., 2015; Carrivick et al., 2015; Capt et al., 2016). With their regular concave topography and dominating stagnant lowering dynamic, les Rognes and Entre la Reille glaciers will likely transform into buried ice patches (Serrano et al., 2011), then talus slopes (Gomez et al., 2003) with the projected future deglaciation context (e.g., Huss and Hock, 2015). Conversely, Tsarmine glacier still retains a flow-dominant dynamic (**Figure 6B**), due to its larger thickness and the presence of a small accumulation area upslope. The studied glaciers thus illustrate distinct stages of debris-covered glacier decay in the negative mass balance periods.

The studied rock glaciers have numerous ridges at their roots, illustrating their probable deformation by glacier advances during positive mass balance periods such as the LIA. These so-called push moraines are very common at the cold glacier margins in permafrost environments (Etzelmüller and Hagen, 2005; Matthews et al., 2014; Dusik et al., 2015). As it currently occurs in the study sites (**Figures 6B**, **7**), differential flow and ablation induce the progressive disconnection between rock glaciers and the upslope glacier zones in negative mass balance periods (Ackert, 1998; Ribolini et al., 2010; Lilleøren et al., 2013). The internal structure to the North of Tsarmine illustrates this situation: a lens of sedimentary ice (distal zone of Tsa-4; **Figure 5**) may have been recently integrated into the distal

former frozen sediments (Tsa-3). Conversely, ice rapidly melts in the concave rooting zone, disconnecting the flowing rock glaciers from the upslope vanishing glacier zones. The long-term individual flow of ice-debris mixtures, weakly sensitive to climatic variations, explains, therefore, the development of rock glaciers at the system margins (Ackert, 1998; Berthling, 2011). This illustrates the morphodynamical continuum that can exist between glacial and periglacial processes, which coexist or follow each other according to climatic variations in these permafrost environments (Benn et al., 2003; Whalley, 2009; Berthling et al., 2013).

CONCLUSION

This study proposes a comprehensive analysis of the relationship between the structure and the current evolution of small debris-covered glaciers located in permafrost environments. The systems studied are complex assemblages of heterogeneous dynamical components, comprised of five sectors associating ice and/or debris in various proportions. Their genesis and organization is related to Holocene climatic fluctuations and illustrate the morphodynamical continuum between glacial and periglacial processes that can exist locally in high mountain environments.

Overall, the same components and dynamics were found in the three sites. The top slopes are almost entirely composed of sedimentary ice, which outcrops or is covered by snow or debris. They experience the most intense and direct responses to climatic variations. The magnitude of surface lowering and downslope motion, a consequence of ice melt, internal deformation and basal sliding, are at least three times higher than in the other sectors. The summer dominant activity shows the noticeable control of warm temperatures and water circulation. In neighboring heavily debris-covered glacier zones of low activity, englacial debris proportion is higher and the supraglacial debris layer is thicker. Consequently, these sectors are less sensitive to the climate and dynamical responses are delayed and attenuated. Active rock glaciers are present in some marginal areas. Their internal structure consists of ice-cored or ice-cemented debris. They experience very low ice melt. The slow flow mainly occurs in winter and progressively detaches them from upslope glaciers. Finally, weakly active ice-free debris are also present.

These results show that direct and high-magnitude responses contrast with delayed and attenuated responses to climate forcing. The variation of ice, debris and water concentration and of the superficial debris layer thickness mainly control this differential evolution. The extended debris cover slows down the ice melt here compared to the rapid decline currently observed in bare-ice glaciers. Their role as local freshwater reservoirs will, therefore, become increasingly important in the next decades. In future research, the results obtained here need to be completed, especially by combining glaciological and geomorphological approaches. In particular, quantification of ice and debris content, hydrological processes and ice origin are avenues worth exploring.

AUTHOR CONTRIBUTIONS

JB and CL designed research. JB conducted field investigations, prepared data, made all figures and wrote the initial version of the paper under the supervision of CL. CL improved the manuscript.

ACKNOWLEDGMENTS

The repeated field investigations would have been impossible to carry out without the help of numerous people. In addition to the authors, during the 38 days of field investigations performed between September 2011 and 2014, 32 other people have contributed to collecting the data synthetized in this article. We sincerely thank them for their indispensable and generous help. We also acknowledge the teams of *Glacier 3000*, *Compagnie du Mont-Blanc*, *Remontées Mécaniques des Houches*, *Refuge du Nid d'Aigle*, *Cabane des Diablerets*, the *municipality of Evolène* and the *Service des forêts et du paysage du Canton du Valais* for logistical support and the Dumas, Katz and Anzévui families for lending local accommodation. This manuscript has been improved thanks to the precious critics and comments of N. Deluigi, A. Tahir, T. Ferber, M. Huss and the two reviewers. M. Blake is acknowledged for proofreading the English text.

REFERENCES

Ackert, R. P. J. (1998). A rock glacier/debris-covered glacier system at Galena Creek, Absaroka Mountains, Wyoming. *Geog. Ann. A.* 80, 267–276. doi: 10.1111/j.0435-3676.1998.00042.x

Anderson, R. S., Anderson, S. P., MacGregor, K. R., Waddington, E. D., O'Neel, S., Riihimaki, C. A., et al. (2004). Strong feedbacks between hydrology and sliding of a small alpine glacier. *J. Geophys. Res.* 109, F03005. doi: 10.1029/2004JF000120

Azócar, G. F., and Brenning, A. (2010). Hydrological and geomorphological significance of rock glaciers in the Dry Andes, Chile (27°-33°S). *Permafrost Periglac. Process.* 21, 42–53. doi: 10.1002/ppp.669

Badoux, H., and Gabus, J. (1991). *Les Diablerets, Atlas Géologique de la Suisse au 1/25 000, 88*. Wabern: Swisstopo.

BAFU (2005). *Hinweiskarte der Potentiellen Permafrostverbreitung in der Schweiz*. Bern: Swiss Federal Office for the Environment.

Benn, D. I., Bolch, T., Hands, K., Gulley, J., Luckman, A., Nicholson, L. I., et al. (2012). Response of debris-covered glaciers in the Mount Everest region to recent warming, and implication for outburst flood hazards. *Earth Sci. Rev.* 114, 156–174. doi: 10.1016/j.earscirev.2012.03.008

Benn, D. I., and Evans, D. J. A. (2010). *Glaciers and Glaciation*. New York, NY: Routledge.

Benn, D. I., Kirkbride, M. P., Owen, L. A., and Brazier, V. (2003). "Glaciated valley landsystems," in *Glacial Landsystems*, ed D. J. A. Evans (*London: Arnold*), 372–406.

Berthling, I. (2011). Beyond confusion: rock glaciers as cryo-conditioned landforms. *Geomorphology* 131, 98–106. doi: 10.1016/j.geomorph.2011.05.002

Berthling, I., Schomacker, A., and Benediktsson, I. Ö. (2013). "The glacial and periglacial research frontier: where from here?" *in Treatise on Geomorphology,* eds J. F. Shroder chief and R. Giardino, and J. Harbor (San Diego, CA: Academic Press), 479–499.

Bingham, R. G., Hubbard, A. L., Nienow, P. W., and Sharp, M. J. (2008). An investigation into the mechanisms controlling seasonal speedup events at a High Arctic glacier. *J. Geophys. Res.* 113, F02006. doi: 10.1029/2007jf000832

Bingham, R. G., Nienow, P. W., Sharp, M. J., and Copland, L. (2006). Hydrology and dynamics of a polythermal (mostly cold) High

Arctic glacier. *Earth Surf. Proc. Land.* 31, 1463–1479. doi: 10.1002/esp.1374

Bodin, X., Schoeneich, P., Lhotellier, R., Gruber, S., Deline, P., Ravanel, L., et al. (2008). "Towards a first assessment of the permafrost distribution in the French Alps," in *Proceedings of the 6th Swiss Geoscience Meeting 2008* (*Lugano*), 175–176.

Boeckli, L., Brenning, A., Gruber, S., and Noetzli, J. (2012). Permafrost distribution in the European Apls: calculation and elevation of an index map and summary statistics. *Cryosphere* 6, 807–820. doi: 10.5194/tc-6-807-2012

Bosson, J. B., Deline, P., Bodin, X., Schoeneich, P., Baron, L., Gardent, M., et al. (2015). The influence of ground ice distribution on geomorphic dynamics since the Little Ice Age in pro-glacial areas of two cirque glacier systems. *Earth Surf. Proc. Land.* 40, 666–680. doi: 10.1002/esp.3666

Brazier, V., Kirkbride, M. P., and Owens, I. F. (1998). The Relationship between climate and rock glacier distribution in the Ben Ohau Range, New Zealand. *Geog. Ann. A.* 80, 193–207. doi: 10.1111/j.0435-3676.1998.00037.x

Capt, M. (2015). *Evolution des Petits Systèmes Glaciaires Situés Dans le Domaine Périglaciaire Alpin à Différentes Échelles Temporelles: Les Cas de Tsarmine (Arolla, Valais) et Entre la Reille (Diablerets, Vaud)*. Master thesis, University of Lausanne.

Capt, M., Bosson, J. B., Fischer, M., Micheletti, N., and Lambiel, C. (2016). Decadal evolution of a small heavily debris-covered glacier located in Alpine permafrost environment. *J. Glaciol.*

Carrivick, J. L., Berry, K., Geilhausen, M., James, W. H. M., Williams, C., Brown, L. E., et al. (2015). Decadal-scale changes of the Ödenwinkelkees, Central Austria, suggest increasing control of topography and evolution towards steady state. *Geog. Ann. A* 97, 543–562. doi: 10.1111/geoa.12100

Carturan, L., Baldassi, G. A., Bondesan, A., Calligaro, S., Carton, A., Cazorzi, F., et al. (2013). Current behavior and dynamics of the lowermost Italian glacier (Montasio Occidentale, Julian Alps). *Geogr. Ann. A.* 95, 79–96. doi: 10.1111/geoa.12002

Clark, D. H., Clark, M. M., and Gillepsie, A. R. (1994). Debris-Covered glaciers in the Sierra Nevada, California, and their implications for snowline reconstructions. *Quat. Res.* 41, 139–153. doi: 10.1006/qres.1994.1016

Cogley, J. G., Hock, R., Rasmussen, L. A., Arendt, A. A., Bauder, A., Braithwaite, R. J., et al. (2011). *Glossary of Glacier Mass Balance and Related Terms.* IHP-VII Technical Documents in Hydrology 86, IACS Contribution 2. Paris: UNESCO-IHP.

Copland, L., Pope, S., Bischop, M. P., Schroder, J. F., Clendon, P., Bush, A., et al. (2009). Glacier velocities across the central Karakoram. *Ann. Glaciol.* 50, 41–49. doi: 10.3189/172756409789624229

Cuffey, K. M., and Paterson, W. S. B. (2010). *The Physics of Glaciers, 4th Edn*. Oxford: Butterworth-Heinemann.

Delaloye, R. (2008). "Parois glaciaires... parois rocheuses: l'évolution séculaire des grandes faces alpines," in *Klimaveränderungen Auf der Spur*, Vol. 5, ed C. Rothenbühler (Samedan: Studien des Europäisches Tourismus Instituts an der Academia Engiadina), 93–104.

Delaloye, R., Perruchoud, E., Avian, M., Kaufmann, V., Bodin, X., Hausmann, H., et al. (2008). "Recent interannual variations of rockglaciers creep in the European Alps," in *Proceedings of the 9th International Conference on Permafrost, 29 June–3 July 2008, Fairbanks, Alaska,* Vol. 1, eds D. L. Kane and K. M. Hinkel (Fairbanks: Institute of Northern Engineering), 343–348.

Deline, P., Gardent, M., Magnin, F., and Ravanel, L. (2012). The morphodynamics of the Mont Blanc massif in a changing cryosphere: a comprehensive review. *Geogr. Ann. A* 94, 265–283. doi: 10.1111/j.1468-0459.2012.00467.x

Deline, P., Gruber, S., Delaloye, R., Fischer, L., Geertsema, M., Giardino, M., et al. (2015). "Ice loss and slope stability in high-mountain regions," in *Snow and Ice-Related Hazards, Risks, and Disasters,* eds J. F. Shroder, W. Haeberli, and C. Whiteman (San Diego, CA: Academic Press), 521–561.

Dobhal, D. (2011). "Glaciers," in *Encylcopedia of Snow, Ice and Glaciers,* eds V. P. Singh, P. Singh, and U. K. Haritashya (Dordrecht: Springer), 376–377.

Dusik, J. M., Leopold, M., Heckmann, T., Haas, F., Hilger, L., Morche, D., et al. (2015). Influence of glacier advance on the development of the multipart Riffeltal rock glacier, Central Austrian Alps. *Earth Surf. Proc. Land.* 40, 965–980 doi: 10.1002/esp.3695

Emmer, A., Loarte, E. C., Klimes, J., and Vilímek, V. (2015). Recent evolution and degradation of the ben Jatunraju glacier (Cordilla Blanca, Peru). *Geomorphology* 228, 345–355. doi: 10.1016/j.geomorph.2014.09.018

Etzelmüller, B., and Hagen, J. O. (2005). "Glacier-permafrost interaction in Arctic and alpine mountain environments with examples from southern Norway and Svalbard," in *Cryospheric Systems: Glaciers and Permafrost*, Vol. 242, eds C. Harris and J. B. Murton (London: Geological Society, Special publications), 11–27.

Evans, D. J. A. (2013). "Geomorphology and retreating glaciers," in *Treatise on Geomorphology,* eds J. F. Shroder chief and, R. Giardino, and J. Harbor (San Diego, CA: Academic Press), 460–478.

Fischer, M., Huss, M., Barboux, C., and Hoelzle, M. (2014). The new Swiss Glacier Inventory SGI2010: relevance of using high-resolution source data in areas dominated by very small glaciers. *Arct. Antarct. Alp. Res.* 46, 933–945. doi: 10.1657/1938-4246-46.4.933

Gardent, M., Rabatel, A., Dedieu, J. P., and Deline, P. (2014). Multitemporal glacier inventory of the French Alps from the late 1960s to the late 2000s. *Glob. Planet. Change* 120, 24–37. doi: 10.1016/j.gloplacha.2014.05.004

Gilbert, A., Vincent, C., Wagnon, P., Thibert, E., and Rabatel, A. (2012). The influence of snow cover thickness on the thermal regime of Tête Rousse Glacier (Mont Blanc range, 3200m a.s.l.): consequences for outburst flood hazards and glacier response to climate change. *J. Geophys. Res.* 117, 165–182. doi: 10.1029/2011JF002258

Gomez, A., Palacios, D., Luengo, E., Tanarro, L. M., Schulte, L., and Ramons, M. (2003). Talus instability in a recent deglaciation area and its relationship to buried ice and snow cover evolution (Picacho del Veleta, Sierra Nevada, Spain). *Geogr. Ann. A* 85, 165–182. doi: 10.1111/1468-0459.00196

Grunewald, K., and Scheithauer, J. (2010). Europe's southernmost glaciers: responses and adaptation to climate change. *J. Glaciol.* 56, 129–142. doi: 10.3189/002214310791190947

Haeberli, W. (2005). "Investigating glacier-permafrost relationships in high-mountain areas: historical background, selected examples and research needs," in *Cryospheric Systems: Glaciers and Permafrost*, Vol. 242, eds C. Harris and J. B. Murton (London: Geological Society, Special Publications), 29–37.

Haeberli, W., Hallet, B., Arenson, L., Elconin, R., Humlum, O., Kääb, A., et al. (2006). Permafrost creep and rock glacier dynamics. *Permafrost Periglac. Process.* 17, 189–214. doi: 10.1002/ppp.561

Haeberli, W., Huggel, C., Paul, F., and Zemp, M. (2013). "Glacial responses to climate change," in *Treatise on Geomorphology,* eds J. F. Shroder chief eds, L. A. James, and C. P. Harend, J. J. Clague (San Diego, CA: Academic Press), 152–175.

Hagg, W., Mayer, C., Lambrecht, A., and Helm, A. (2008). Sub-debris melt rates on southern Inylchek Glacier, central Tian Shan. *Geogr. Ann. A* 90, 55–63. doi: 10.1111/j.1468-0459.2008.00333.x

Hauck, C., and Kneisel, C. (eds.). (2008). *Applied Geophysics in Periglacial Environments. Cambridge: Cambridge University Press.*

Hauck, C., Vonder Mühll, D., and Maurer, H. (2003). Using DC resistivity tomography to detect and characterize mountain permafrost. *Geophys. Prospect.* 51, 273–284. doi: 10.1046/j.1365-2478.2003.00375.x

Hausmann, H., Krainer, K., Brückl, E., and Mostler, W. (2007). Internal structure and ice content of Reichenkar rock glacier (Stubai Alps, Austria) assessed by geophysical investigations. *Permafrost Periglac. Process.* 18, 351–367. doi: 10.1002/ppp.601

Hilbich, C., Marescot, L., Hauck, C., Loke, M. H., and Mäusbacher, R. (2009). Applicability of Electrical Resistivity Tomography Monitoring to Coarse Blocky and Ice-rich Permafrost Landforms. *Permafrost Periglac. Process.* 20, 269–284. doi: 10.1002/ppp.652

Huss, M., and Hock, R. (2015). A new model for global glacier change and sea-level rise. *Front. Earth Sci.* 3:54. doi: 10.3389/feart.2015.00054

Isaksen, K., Ødegård, R. S., Eiken, T, and Sollid, J. L. (2000). Composition, flow and development of two tongue-shaped rock glaciers in the permafrost of Svalbard. *Permafrost Periglac. Process.* 11, 241–257. doi: 10.1002/1099-1530(200007/09)11:3<241::AID-PPP358>3.0.CO;2-A

Ivy-Ochs, S., Kerschner, H., Maisch, M., Christl, M., Kubik, P., and Schlüchter, C. (2009). Latest pleistocene and holocene glacier variations in the European Alps. *Quat. Sci. Rev.* 28, 2137–2149. doi: 10.1016/j.quascirev.2009.03.009

Janke, J. R., Bellisario, A., and Ferrando, F. A. (2015). Classification of debris-covered glaciers and rock glaciers in the Andes of central Chile. *Geomorphology* 241, 98–121. doi: 10.1016/j.geomorph.2015.03.034

Kääb, A., Haeberli, W., and Gudmundsson, G. H. (1997). Analysing the creep of mountain permafrost using high precision aerial photogrammetry: 25 years

of monitoring gruben rock Glacier, Swiss Alps *Permafrost Periglac. Process.* 8, 409–426.

Kirkbride, M. P. (2011). "Debris-covered glaciers," in *Encylcopedia of Snow, Ice and Glaciers,* eds V. P. Singh, P. Singh, and U. K. Haritashya (Dordrecht: Springer), 190–192.

Kirkbride, M. P., and Deline, P. (2013). The formation of supraglacial debris covers by primary dispersal from transverse englacial debris bands. *Earth Surf. Proc. Land.* 15, 1779–1792. doi: 10.1002/esp.3416

Kirkbride, M. P., and Warren, C. R. (1999). Tasman Glacier, New Zealand: 20th-century thinning and predicted calving retreat. *Glob. Planet. Change* 22, 11–28. doi: 10.1016/s0921-8181(99)00021-1

Kneisel, C. (2003). Permafrost in recently deglaciated glacier forefields - measurements and observations in the eastern Swiss Alps and northern Sweden. *Z. Geomorph. N. F.* 47, 289–305.

Kneisel, C., and Kääb, A. (2007). Mountain permafrost dynamics within a recently exposed glacier forefield inferred by a combined geomorphological, geophysical and photogrammetrical approach. *Earth Surf. Proc. Land.* 32, 1797–1810. doi: 10.1002/esp.1488

Knight, J., and Harrison, S. (2014). Mountain glacial and paraglacial environments under global climate change: lessons from the past, future directions and policy implications. *Geogr. Ann. A* 96, 245–264. doi: 10.1111/geoa.12051

Kuhn, M. (1995). The mass balance of very small glaciers. *Z. Gletscherkd. Glazialgeol. 31*, 171–179.

Lambiel, C., Bardou, E., Delaloye, R., Schuetz, P., and Schoeneich, P. (2009). Extension spatiale du pergélisol dans les Alpes vaudoises: implication pour la dynamique sédimentaire locale. *Bull. Soc. Vaudoise Sci. Nat.* 91, 407–424.

Lambiel, C., and Delaloye, R. (2004). Contribution of real-time kinematic GPS in the study of creeping mountain permafrost: examples from the Western Swiss Alps. *Permafrost Periglac. Process.* 15, 229–241. doi: 10.1002/ppp.496

Lambiel, C., Reynard, E., Cheseaux, G., and Lugon, R. (2004). Distribution du pergélisol dans un versant instable, le cas de Tsarmine (Arolla, Evolène, Vs). *Bull. Murithienne.* 122, 89–102.

Lambrecht, A., Mayer, C., Hagg, W., Popovnin, V., Rezepkin, A., Lomidze, N., et al. (2011). A comparison of glacier melt on debris-covered glaciers in the northern and southern Caucasus. *Cryosphere* 5, 525–538. doi: 10.5194/tc-5-525-2011

Lilleøren, K. S., Etzelmüller, B., Gärtner-Roer, I., Kääb, A., Westermann, S., and Gudmundsson, A. (2013). The distribution, thermal characteristics and dynamics of permafrost in tröllaskagi, northern iceland, as inferred from the distribution of rock glaciers and ice-cored moraines. *Permafrost Periglac. Process.* 24, 322–335. doi: 10.1002/ppp.1792

Maisch, M., Haeberli, W., Hoelzle, M., and Wenzel, J. (1999). Occurrence of rocky and sedimentary glacier beds in the Swiss Alps as estimated from glacier-inventory data. *Ann. Glaciol.* 43, 232–235. doi: 10.3189/172756499781821779

Matthews, J. A., Winkler, S., and Wilson, P. (2014). Age and origin of ice-cored moraines in jotunheimen and breheimen, southern norway: insights from schmidt-hammer exposure-age dating. *Geog. Ann. A.* 96, 531–548. doi: 10.1111/geoa.12046

Mattson, L. E. (2000). "The influence of a debris cover on the mid-summer discharge of Dome Glacier, Canadian Rocky Mountains," in *Debris-Covered Glaciers,* Vol. 264, eds M. Nakawo, C. F. Raymond, and A. Fountain (Seattle, WA: IAHS Publication), 25–33.

Mayer, C., Lambrecht, A., Belò M., Smiraglia, C., and Diolaiuti, G. (2006). Glaciological characteristics of the ablation zone of Baltoro glacier, Karakorum, Pakistan. *Ann. Glaciol.* 43, 123–131. doi: 10.3189/172756406781812087

Mennessier, G., Rosset, F., Bellière, J., Dhellemmes, R., Oulianoff, N., Antoine, P., et al. (1976). *St-Gervais-les-Bains, Carte Géologique de la France à 1/50 000, 703.* Orléans: BRGM.

Micheletti, N., Lambiel, C., and Lane, S. N. (2015). Investigating decadal scale geomorphic dynamics in an Alpine mountain setting. *J. Geophys. Res.* 120, 2155–2175. doi: 10.1002/2015JF003656

Monnier, S., and Kinnard, C. (2015). Reconsidering the glacier to rock glacier transformation problem: new insights from the central Andes of Chile. *Geomorphology* 238, 47–55. doi: 10.1016/j.geomorph.2015.02.025

Monnier, S., Kinnard, C., Surazakov, A., and Bossy, W. (2014). Geomorphology, internal structure, and successive development of a glacier foreland in the semiarid Chilean Andes (Cerro Tapado, upper Elqui Valley, 30°08′ S., 69°55′ W.). *Geomorphology* 207, 126–140. doi: 10.1016/j.geomorph.2013.10.031

Nicholson, L., and Benn, D. I. (2006). Calculating ice melt beneath a debris layer using meteorological data. *J. Glaciol.* 52, 463–470. doi: 10.3189/172756506781828584

Paasche, Ø. (2011). "Cirque glaciers," in *Encylcopedia of Snow, Ice and Glaciers,* eds V. P. Singh, P. Singh, and U. K. Haritashya (Dordrecht: Springer), 141–144.

Paul, F., Kääb, A., and Haeberli, W. (2007). Recent glacier changes in the Alps observed by satellite: consequences for future monitoring strategies. *Glob. Planet. Change* 56, 111–122. doi: 10.1016/j.gloplacha.2006.07.007

Pfeffer, W. T., Arendt, A. A., Bliss, A., Bolch, T., Cogley, J. G., Gardner, A. S., et al. (2014). The Randolph Glacier Inventory: a globally complete inventory of glaciers. *J. Glaciol.* 221, 537–552. doi: 10.3189/2014JoG13J176

Pourrier, J., Jourde, H., Kinnard, C., Gascoin, S., and Monnier, S. (2014). Glacier meltwater flow paths and storage in a geomorphologically complex glacial foreland: the case of the Tapado glacier, dry Andes of Chile (30° S). *J. Hydrol.* 519, 1068–1083. doi: 10.1016/j.jhydrol.2014.08.023

Rangecroft, S., Harrison, S., and Anderson, K. (2015). Rock Glaciers as water stores in the bolivian andes: an assessment of their hydrological importance. *Arct. Antarct. Alp. Res.* 47, 89–98. doi: 10.1657/AAAR0014-029

Reynard, E., Delaloye, R., and Lambiel, C. (1999). Prospection géoélectrique du pergélisol alpin dans le massif des Diablerets (VD) et au Mont Gelé (Nendaz, Vs). *Bull. Murithienne.* 117, 89–103.

Reynard, E., Lambiel, C., Delaloye, R., Devaud, G., Baron, L., Chapellier, D., et al. (2003). "Glacier/permafrost relationships in forefields of small glaciers (Swiss Alps)," in *Proceedings of the 8th International Conference on Permafrost*, Vol. 1, eds M. Phillips, S. M. Springman, and L. U. Arenson *(Zurich)*, 947–952.

Ribolini, A., Guglielmin, M., Fabre, D., Bodin, X., Marchisio, M., Sartini, S., et al. (2010). The internal structure of rock glaciers and recently deglaciated slopes as revealed by geoelectrical tomography: insights on permafrost and recent glacial evolution in the Central and Western Alps (Italy-France). *Quat. Sci. Rev.* 29, 507–521. doi: 10.1016/j.quascirev.2009.10.008

Rippin, D. M., Willis, I. C., Arnold, N. S., Hodson, A. J., and Brinkhaus, M. (2005). Spatial and temporal variations in surface velocity and basal drag across the tongue of the polythermal glacier midre Lovénbreen, Svalbard. *J. Glaciol.* 51, 588–600. doi: 10.3189/172756505781829089

Scherler, D., Bookhagen, B., and Strecker, M. R. (2011). Spatially variable response of Himalaysan glaciers to climate change affected by debris cover. *Nat. Geosci.* 4, 156–159. doi: 10.1038/ngeo1068

Schomacker, A., and Kjær, K. H. (2007). Origin and de-icing of multiple generations of ice-cored moraines at Bruarjökull, Iceland. *Boreas* 36, 411–425. doi: 10.1080/03009480701213554

Seppi, R., Zanoner, T., Carton, A., Bondesan, A., Frances, R., Carturan, L., et al. (2015). Current transition from glacial to periglacial processes in the Dolomines (South-Eastern Alps). *Geomorphology* 228, 71–86. doi: 10.1016/j.geomorph.2014.08.025

Serrano, E., González-Trueba, J. J., Sanjosé J. J., and Del Rìo, L. M. (2011). Ice patch origin, evolution and dynmics in a temperate high mountain environment: the Jou Negro, Picos de Europoa (NW Spain). *Geogr. Ann. A* 93, 57–70. doi: 10.1111/j.1468-0459.2011.00006.x

Shroder, J. F., Bishop, M. P., Copland, L., and Sloan, V. F. (2000). Debris-covered glaciers and rock glaciers in the Nanga Parbat Himalya, Pakistan. *Geogr. Ann. A* 82, 17–31. doi: 10.1111/j.0435-3676.2000.00108.x

WGMS (2008). *Global Glacier Changes: Facts and Figures*, eds M. Zemp, I. Roer, A. Kääb, M. Hoelzle, F. Paul, W. Haeberli (Zurich: UNEP and World Glacier Monitoring Service).

Whalley, W. B. (2009). "On the interpretation of discrete debris accumulations associated with glaciers with special reference to the British Isles," in *Periglacial and Paraglacial Processes and Environments,* Vol. 320, eds J. Knight and S. Harrison (London: Geological Society, Special publications), 85–102.

Zemp, M., Frey, H., Gärtner-Roer, I., Nussbaumer, S. U., Hoelzle, M., Paul, F., et al. (2015). Historically unprecedented global glacier decline in the earlly 21st century. *J. Glaciol.* 228, 745–762. doi: 10.3189/2015JoG15J017

Conflict of Interest Statement: The authors declare that the research was conducted in the absence of any commercial or financial relationships that could be construed as a potential conflict of interest.